Journal of Membrane Science 526 (2017) 301–314

Contents lists available at ScienceDirect

Journal of Membrane Science

journal homepage: www.elsevier.com/locate/memsci

# Phase separation analysis of Extem/solvent/non-solvent systems and relation with membrane morphology

Saeed Mazinani[a,*], Siavash Darvishmanesh[b], Arash Ehsanzadeh[a], Bart Van der Bruggen[a]

[a] ProcESS - Process Engineering for Sustainable Systems, Department of Chemical Engineering, KU Leuven, Celestijnenlaan 200F, B-3001 Leuven, Belgium
[b] Department of Chemical and Biological Engineering, Princeton University, Princeton, New Jersey 08544, USA

ARTICLE INFO

*Keywords:*
Ternary phase diagram
Binodal curve
Extem
Coagulant
Membrane morphology

ABSTRACT

The phase separation behavior of Extem/water/solvent systems for various solvents and Extem/NMP/non-solvent systems for different types of coagulants was investigated. Ternary phase diagrams of studied systems were constructed based on cloud point data obtained by titration at room temperature. In the first part, N-methyl-2-pyrrolidone (NMP), dimethylacetamide (DMAc), dimethylformamide (DMF) and dimethyl sulfoxide (DMSO) were employed as solvent and water was used as coagulant. The cloud point curves from these systems showed that Extem/NMP/water and Extem/DMSO/water has the smallest and largest demixing gap, respectively. Subsequently, water, methanol, and glycerol were employed as coagulants and NMP was selected as solvent. The obtained results indicated that water and methanol had the strongest and weakest coagulant power, respectively. The linearized cloud point and precipitation value were applied to identify the strength of the non-solvent for casting solution (Extem/NMP) with a certain concentration. The solubility curve of Extem was obtained using the Hansen solubility parameter, calculated by a group contribution method. In order to evaluate the influence of different solvents and non-solvents on the final structure of the resulting membranes, scanning electron microscopy (SEM) was used. The morphology of the membranes prepared from Extem/solvent/water systems (except Extem/DMSO/water) showed a finger like sub-layer, while a sponge-like structure was observed for the Extem/DMSO/water system. Using methanol as coagulation medium resulted in a thick dense layer over a macroporous sub layer, while a fully sponge like structure with microporous skin layer was obtained for the Extem/NMP/glycerol system. In order to find the source of these unexpected observations, thermodynamic and kinematic aspects such as binary interaction parameters, heat of mixing, viscosity and diffusion rate were discussed thoroughly.

## 1. Introduction

Phase inversion (phase separation), as a well-known method, is used for the preparation of polymeric membranes that can be applied in various processes and applications such as gas separation, water treatment, the biochemical and pharmaceutical industry, etc. The preparation of asymmetric membranes can be accomplished by several techniques which non-solvent induced phase separation (NIPS) is the most industrially used method [1–5]. In NIPS, a homogeneous polymer solution containing a polymer and a relevant solvent is first casted as a flat film on a suitable support, shortly exposed to air, then immersed in a coagulation medium that acts as a non-solvent for the membrane casting solution. The so formed membrane typically has an asymmetric structure including a thin, selective top layer over a porous sublayer. It should be noted that if water vapor is absorbed by the casting solution, phase separation can take already place, as applied in the so called vapor-induced phase separation (VIPS) technique [6–8]. Generally, structure of the membrane is controlled by both the thermodynamic and the kinetic aspects of the membrane forming system. The thermodynamic part of the system is defined by the phase equilibrium between components while the kinetic part is related to the mutual diffusion between components [9–11].

The ternary phase diagram plays a key role in defining the final morphological and microstructure of the membrane. Since a phase diagram is constructed based on thermodynamic characterization of the system, it shows a qualitative description of the thermodynamic features of the membrane formation process. In addition, ternary phase diagrams can clearly demonstrate whether a certain polymer/solvent/non-solvent system forms a membrane with specific structure [12,13]. Therefore, in order to improve asymmetric membranes, a comprehensive analysis of the phase separation behavior of a casting solution in the presence of a non-solvent is essential. Fig. 1 shows the

* Corresponding author.
*E-mail address:* saeed.mazinani@kuleuven.be (S. Mazinani).

http://dx.doi.org/10.1016/j.memsci.2016.12.031
Received 30 October 2016; Received in revised form 15 December 2016; Accepted 18 December 2016
Available online 20 December 2016
0376-7388/ 

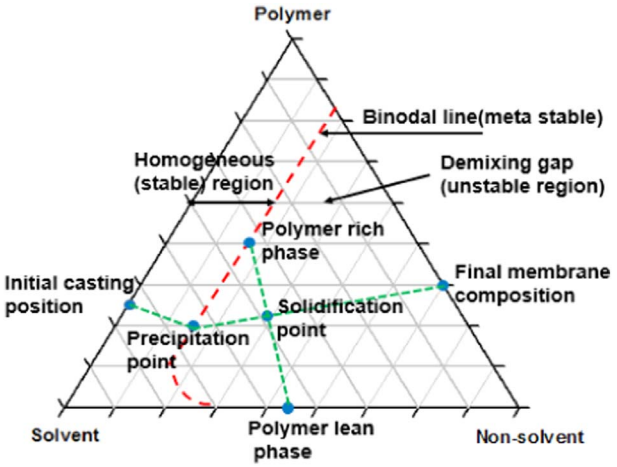


**Fig. 1.** Schematic phase diagram of the ternary system during membrane formation.

ternary phase diagram and composition path of the polymer solution during precipitation process. The ternary diagram is divided into two regions by the cloud point curve: a homogenous stable region where all species are present in a single phase, and a two phase region where the system is divided into separate phases, a polymer rich and a polymer lean phase, which are in thermodynamic equilibrium.

In a ternary system, every composition on the cloud point curve (meta-stable region) demixes into two separate phases (of course with different compositions) but that are in equilibrium. The membrane formation is tracked from the initial casting solution to the final solid structure through the composition path. The precipitation point is the point that the polymer precipitation starts. As the precipitation continues, the polymer viscosity increases to becomes high, and is considered a solid. Composition of polymer, solvent and non-solvent in each separated phase at equilibrium state can be determined by a tie line passing through the solidification point. Thus, the initial composition of the polymer solution, the position of the binodal line and the composition pathway have a profound effect on the membrane morphology [14,15]. It should be noted that in macromolecular systems, equilibrium always does not occur, while as mentioned above the phase diagram presents an equilibrium state. Hence, the phase separation in these systems is affected by kinetic parameters as well [16,17]. Although kinetics of transport process influence the membrane final structure, thermodynamic analysis of phase separation is still the main interest of many researchers. For example, Kim et al. [18] evaluated the phase separation and corresponding membrane structure of Matrimid/DMSO/water and Matrimid/NMP/water systems at room temperature. They determined the ternary phase diagram including the binodal and spinodal curves, gelation point, and tie-lines. The cloud point curve of Matrimid/DMSO/water system was much closer to the polymer-solvent axis compared to Matrimid/NMP/water. The opposite result was observed by SEM images. A finger-like structure was obtained for Matrimid/NMP/water system while the Matrimid/DMSO/water system exhibited a sponge-like (free macrovoid) membrane. It was found that in the Matrimid/DMSO/water system, the membrane morphology is determined at an earlier stage than in the Matrimid/NMP/water system, resulting in a sponge-like structure. Wang and Teo [19] analyzed the phase separation behavior of Ultem/solvent/non-solvent systems for different solvents and non-solvents through the measurement of precipitation values (PVs) at temperatures between 20 and 50 °C. The hollow-fiber membranes prepared from a solvent with higher PV showed a dense skin layer, while a porous skin layer was observed from a solvent with much lower PV. Leblanc et al. [20] experimentally determined the ternary phase diagram of a fluorinated polyimide (6FDA-mPDA) by using different solvents and non-solvents at 20 °C. They also evaluated the morphology of membranes prepared from a 6FDA-mPDA/solvent/non-solvent systems by SEM to examine the correlation with the membrane morphology. The comparison of SEM images showed that the local polymer concentration is the most important factor for membrane formation, which is directly related to the thermodynamic and kinetic parameters. Barzin and Sadatnia [21] investigated the phase separation and membrane morphologies of PES/DMAc/water and PES/NMP/water systems at room temperature. An instantaneous liquid-liquid demixing was induced for both systems; this typically results in macrovoids occurrence. Despite the lower miscibility (higher interaction parameter) between water/NMP compared to water/DMAc, the membranes prepared from the water/NMP system showed less sponge-like structures. They discovered that the type of macrovoid structures is significantly affected by the position of vitrification and gelation boundaries. Yin et al. [22] analyzed theoretically the phase behavior of three systems including polyamic acid (PAA)/DMAc/water, PAA/DMAc/ethylene glycol (EG) and PAA/DMAc/ethanol. The surface and cross-section structures of the fibers were also investigated by SEM. This indicated that an increasing DMAc amount in the coagulation bath generates sponge-like with rough surfaces, while further increasing the DMAc concentration led to porous structures.

In the current study, we attempted to comprehensively analyse the phase separation behavior of Extem/solvent/non-solvent systems with various solvents and non-solvents and to relate thermodynamic and kinetic parameters of the studied systems with their membrane morphologies. To the best our knowledge, no research is available in the literature on the phase separation behavior of Extem/solvent/non-solvent systems. Thermodynamic phase diagrams of Extem/solvent/non-solvent systems for different solvents and coagulations were constructed by cloud point measurement at room temperature. The solubility region (solubility envelope) of Extem was identified based on Hansen solubility parameters, calculated through group contribution. In order to identify the non-solvent strength for the casting solution (Extem/NMP), the linearized cloud point (LCP) and PV were employed. The morphology of asymmetric flat sheet membranes was examined by SEM to evaluate the effect of various solvents and coagulants on the final structures of membranes. The reason for selecting Extem as the polymer is that it is a relatively new aromatic polyetherimide with ether (–O–), isopropylidene (–$C(CH_3)_2$–) and sulfone (S=O) groups, which has an excellent performance up to high temperatures with a superior resistance to chemicals including organics and acids, a high thermal-oxidative stability and good processability [23]. This makes it a good candidate for membrane processes like gas separation, organic solvent nanofiltration and pervaporation in harsh environments. The structure of Extem is shown in Fig. 2.

## 2. Experimental

### 2.1. Choice of solvents and non-solvents

In phase inversion process, the choice of a solvent/non-solvent combination has a profound effect on the morphology, mechanical properties and separation performance of asymmetric membranes [5,24]. The choice of a solvent is actually depends on the selection of the polymer, since the polymer must readily dissolvable or dispersible in the selected solvent.

NMP, DMF, DMAc, and DMSO were employed as the solvents for the dope formulation due to their high miscibility with water; they have a different degree of interaction with the polymer (Extem). However, it is not easy to evaporate those solvents from the casting solution due to their poor volatilities. Therefore, vacuum evaporation, high temperature evaporation, or a prolonged evaporation period should be applied.

Before the selection of the coagulants, it should be noted that the solvent and the non-solvent must be completely miscible. Deionized water was used as an inexpensive and environmentally safe coagulant. Methanol and glycerol were also selected as non-solvents due to their

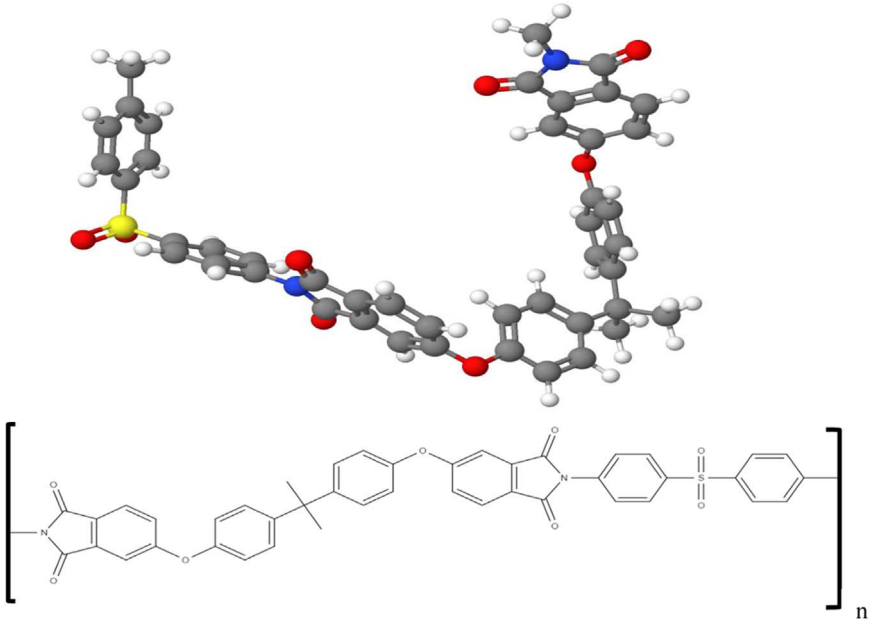

**Fig. 2.** The chemical structure of Extem [23].

miscibility properties.

### 2.2. Materials

Extem was kindly supplied by SABIC (Lommel, Belgium). The solvents were purchased from Acros Chemical Company (Geel, Belgium) with a purity higher than 99%. Glycerol and methanol ( > 99.5%), used as non-solvents, were obtained from Merck. The solvents and non-solvents were used for preparation of polymer solutions without further purification.

### 2.3. Preparation of dope solution

Extem was dried out overnight in a vacuum oven at 200 °C prior to use to remove possible residual moisture. Then, it was dissolved in the desired solvent and stirred for 2 days at 60 °C. Polymer solutions were prepared in closed Duran® glass bottles and sealed by Parafilm® to avoid either solvent evaporation or water sorption to the solution. The prepared solutions were filtered by using filter paper (Whatman) to obtain a clear and homogenous solution.

### 2.4. Preparation of flat sheet asymmetric membranes

The homogeneous casting solutions with a concentration of 25 wt% were cast uniformly on a glass plate by using an automated film applicator (Braive Instruments, Belgium) operating in a casting box and equipped with a humidity sensor controlling the humidity during the casting. The nascent polymer films were exposed to air for period of 10 s. Right after this short solvent evaporation, it was immersed into the non-solvent bath. The temperature of non-solvent bath was adjusted to the ambient temperature. The phase separation between desired solvent and non-solvent happens instantly, turning the polymer solution from transparent to turbid. The membranes were kept for 48 h more to remove all solvents. To remove residual solvents, to protect the fine dense selective layer, and to avoid pore collapsing due to the large capillary forces during drying of the membrane, a low surface tension liquid (methanol) was then solvent-exchanged for 4 h. Finally, the membranes were washed (deionized water) and then dried in the air.

### 2.5. Cloud point measurements

Simple titration was used to obtain the ternary phase diagram of Extem/solvent/non-solvent systems. Titration is a relatively quick and commonly used technique for determination of the cloud point curve [25]. First, polymer (Extem) was dissolved in a desired solvent and stirred for 2 days to forms a clear, and homogeneous polymer solution which is thermodynamically stable. Then, a certain amount of polymer solution (5–10 g) is placed in a glass vessel at ambient temperature. After that, small amount of pure non-solvent or a solvent/non-solvent mixture with known compositions were added drop-wise to the mechanically stirred polymer solution by using a 5 ml syringe until turbidity was visually observed. The cloud point was allocated when the turbidity of the solution remained for 30 min. It should be mentioned that when the solution is opaque, it separates into two phases and liquid-liquid demixing is induced. With an increasing amount of non-solvent, the polymer is partially precipitated and polymer solution become solid. Next, the polymer solution was diluted with the solvent and eventually becomes clear (one-phase); the experiment was then repeated. The composition of the polymer at the moment can be calculated by the total amounts of polymer, solvent and non-solvent present. Actually, the amount of non-solvent that is required to precipitate the polymer solution offers a rough estimate of the interaction parameter [8,25,26].

### 2.6. Scanning electron microscopy (SEM)

The morphological characteristics of the asymmetric flat sheet membranes were analyzed using a scanning electron microscope (XL30 FEG, SEM Philips). Before SEM examination, samples were placed in an oven overnight. Then, they were soaked in hexane, which helps to freeze the samples and ensure a smooth cut. Subsequently, liquid nitrogen was used for fracturing the samples and to avoid smearing the cross-section of the membranes.

### 2.7. Viscosity measurements

The viscosity of casting solutions were measured by using a stress-controlled mcr501 rheometer (Anton Paar, USA) using a cone-plate configuration with cone angle of 1° and diameter of 50 mm at shear

rate between 0 and 10 1/s. The temperature was set to 25 °C and an evaporation blocker was used to prevent evaporation of the solvent.

## 3. Results and discussion

### 3.1. Solubility envelope of Extem

Solubility of a given polymer in a certain solvent is promoted (higher interaction parameter) if the solubility parameters of polymer and solvent are equal or very similar [27]. The polymer solubility region, denoted as the “solubility envelop” or “solubility map”, can be used to select a suitable solvent (also non-solvent) for preparation of casting solutions. Based on a method developed by Hansen, the solubility envelop for a polymer is used to identify the solubility behavior of the polymer in a number of solvents with varying degrees of dispersion (non-polarity), polarity and hydrogen-bonding character. In the solubility space, solubility envelops of polymer is deduced by developing a sphere around the solvents which can dissolve the polymer. The center of sphere indicates the individual solubility parameters of the polymer. The position of this envelope is identified by the change from soluble to insoluble. Inside the envelope most solvents dissolve the polymer; outside the envelope most solvents cannot dissolve the polymer [28,29]. Three-dimensional and two-dimensional coordinates of solubility parameters are used to determine the solubility envelope for a certain polymer. The three-dimensional representation of the solubility parameters developed by Hansen includes dispersion ($\delta_v$), polar ($\delta_p$) and hydrogen-bonding ($\delta_h$). A more simple approach to solubility parameters usually includes hydrogen and polar bonding. Another approach to develop the polymer solubility envelop in two dimensions using all three solubility parameter is introduced by Bagley et al. [30]. In this method the dispersion and polar solubility parameter is merged to form a new parameter $\delta v$ ($\delta^2 v = \delta^2 d + \delta^2 p$). A two dimensional diagram based on $\delta h$ and $\delta v$ is plotted and used to find the solubility envelop of a polymer.

The solubility region can be approximated by a circle with a radius of about 5 δ-units. In general, Extem is soluble in solvents for which:

$$\sqrt{(\delta_v - 18)^2 + (\delta_h - 5)^2} < 5 \quad (1)$$

The solubility parameter diagram of $\delta_h$ versus $\delta_v$ of the solvents and non-solvents used is shown in Fig. 3. The detailed calculation of the Hansen solubility parameter for polymer is explained in Appendix A.

It is clear from Fig. 3 that Extem is soluble in aprotic solvents like NMP, DMSO, DMF and DMAC. According to the solubility parameter concept, the solvents near the solubility envelope are strong swelling agents for the polymer. For the solvents positioned in the upper right area, no interaction with the polymers is expected because this area is far away from the envelope where the solvents are located [31].

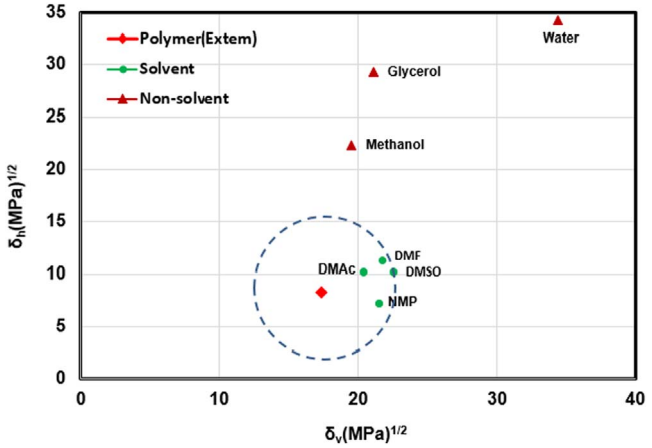


**Fig. 3.** The solubility envelope of Extem.

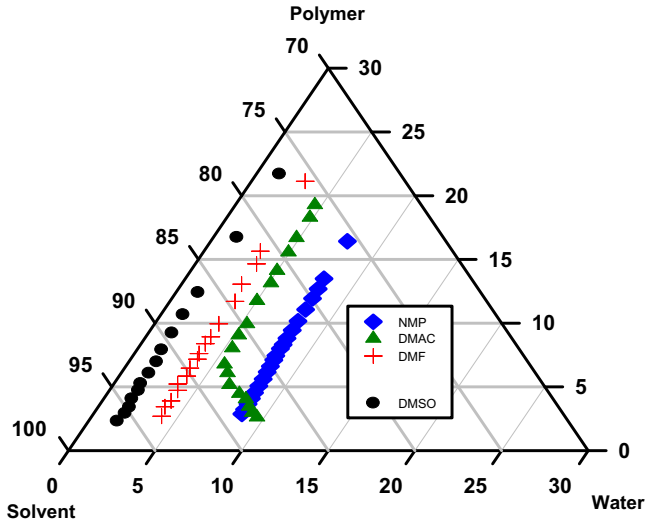


**Fig. 4.** The cloud point lines of water/solvent/Extem systems at room temperature.

Water and glycerol are considered strong non-solvents for membrane formation while methanol can be considered a weak non-solvent. Due to the qualitative nature of the method, determination of the exact solubility boundaries is difficult. However, with a good approximation, the solvents that are within the solubility envelop can dissolve or swell the polymer significantly [32].

### 3.2. Ternary phase diagram of Extem/solvent/water systems

The position of the binodal line is one of the most important features in a ternary phase diagram, which is determined by the interactions between the components, and represented by three binary interaction parameters: non-solvent/solvent ($g_{12}$), polymer/solvent ($\chi_{32}$), polymer/non-solvent ($\chi_{31}$). These interaction parameters involve both enthalpy and entropy contributions [33,34]. The experimental cloud point data for water/DMAc/Extem, water/NMP/Extem, water/DMF/Extem and water/DMSO/Extem at room temperature are shown in Fig. 4. A polymer (Extem) concentration of 25% was used since this concentration range can cover most polymer concentrations usually applied for membrane formation. The polymer concentration varies between 25% and 3% which typically cloud points in this range are placed on a straight line with small difference. The cloud point detection at low polymer concentration (below 3%) is not very precise.

Among the studied systems, the cloud point curve of water/DMSO/Extem was found the closest to the polymer-solvent axis, which represents the largest demixing gap, while the cloud point curve of water/NMP/Extem is the closest to the polymer-non-solvent axis, which indicates that it has the smallest demixing gap. The difference between the cloud point lines of Extem/solvent/water systems can be interpreted by considering the interactions between the components.

It is believed that $g_{12}$ has the most significant effect on the demixing behavior and thus on the location of the binodal line [35–37]. The interaction parameters between non-solvent/solvent are shown in Fig. 5. It can be seen that the water/DMSO system has the lowest interaction value (negative over the entire composition range), which indicates a good miscibility between water/DMSO in comparison with other water/solvent systems in the order: DMSO > DMF > DMAc > NMP. It can be seen that as the amount of solvent in water/solvent mixtures decreases, $g_{12}$ value decreases.

Polymer/solvent interaction can also have a significant effect on the location of the binodal line. It was shown that a polymer/solvent pair with a high mutual affinity (low $\chi_{32}$) has a smaller demixing gap especially at high values of $g_{12}$ [36,37]. The affinity between polymer and solvent is mainly determined by solubility parameters. Hansen

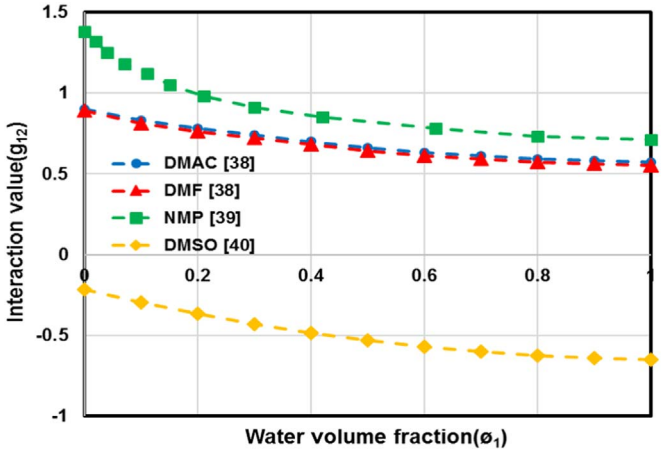


**Fig. 5.** Concentration-dependency of water/solvent interaction parameters at 25 °C [38–40].

[27] applied the following equation for the prediction of interaction parameters between polymer and solvent:

$$\chi_{sp} = \alpha\frac{v_s}{RT}[(\delta_{dp} - \delta_{ds})^2 + 0.25(\delta_{pp} - \delta_{ps})^2 + 0.25(\delta_{hp} - \delta_{hs})^2] \quad (2)$$

where $v_s$ is the molar volume of solvent ($cm^3$/mole), $R$ is the gas constant ($cm^3$ MPa $K^{-1}$ $mol^{-1}$) and $T$ is the absolute temperature (K). The optimum value of the correction constant α is 0.6, as estimated by Lindvig et al. [41]. Table 1 presents the Hansen solubility parameters of the polymer and selected solvents.

The interaction parameters between the polymer (Extem) and solvents used are tabulated in Table 2. The strength of the interaction parameter between Extem and selected solvents are in the order: DMAc > NMP > DMF > DMSO. Thus, DMAc and DMSO have the strongest and weakest interactions with Extem, respectively.

As was expected, the influence of the non-solvent/solvent interaction is more important than that of the polymer/solvent interaction and minimizes the effect of the latter. The higher value of χ for the water/NMP system causes a broader homogeneous (stable) area for this system in comparison with other water/solvent systems. The size of the demixing gap reflects the amount of non-solvent needed for precipitation of the polymer solution. The length of this area in the graph indicates that the solvent dissolution power for Extem/solvent/water ranks: NMP > DMAc > DMF > DMSO. Consequently, for Extem/DMSO less water is needed for phase separation in comparison with other Extem/solvent systems. This thermodynamic analysis can be used for choosing suitable solvents in membrane manufacturing. However, the membrane formation is affected by both thermodynamic and kinetic aspects of the membrane forming system.

### 3.3. Ternary phase diagram of Extem/NMP/non-solvent

Besides the use of a different solvent, a change in the non-solvent also significantly influences the demixing phenomena. In ternary systems, the location of the liquid-liquid demixing gap is significantly determined by the non-solvent/polymer interaction ($\chi_{13}$) [42,43]. The influence of the non-solvent on liquid-liquid phase separation was studied for Extem/NMP/non-solvent. The experimental cloud point data for Extem/NMP/water, Extem/NMP/methanol and Extem/NMP/glycerol systems have been illustrated in Fig. 6. The NMP/methanol system showed the smallest demixing gap among the NMP/non-solvent systems in the following order: NMP/methanol < NMP/glycerol < NMP/water.

**Table 1**
The Hansen solubility parameters for polymer and selected solvents [31].

| Solvents | $\delta_D$ $(MPa)^{1/2}$ | $\delta_P$ $(MPa)^{1/2}$ | $\delta_h$ $(MPa)^{1/2}$ | $\delta_t$ $(MPa)^{1/2}$ |
|---|---|---|---|---|
| Extem | 17.01 | 3.66 | 8.27 | 19.27 |
| NMP | 17.9 | 12.3 | 7.2 | 22.95 |
| DMAc | 16.8 | 11.5 | 10.2 | 22.77 |
| DMF | 17.4 | 13.7 | 11.3 | 24.86 |
| DMSO | 18.4 | 16.4 | 10.2 | 26.67 |

**Table 2**
Interaction parameters between Extem and selected solvents.

| Polymer | $\chi_{sp}$ (NMP) | $\chi_{sp}$ (DMSO) | $\chi_{sp}$ (DMAc) | $\chi_{sp}$ (DMF) |
|---|---|---|---|---|
| Extem | 0.41 | 0.51 | 0.32 | 0.46 |

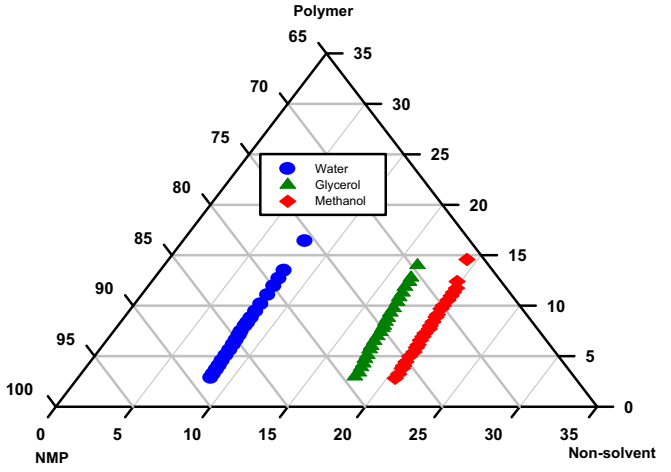


**Fig. 6.** The cloud point lines of non-solvent/NMP/Extem systems at room temperature.

Because the interactions of NMP/water and NMP/methanol systems are almost similar [44], the difference between cloud point lines of Extem/NMP/non-solvents systems can be explained by considering the polymer/non-solvent ($\chi_{13}$) interaction parameter. If the cloud point curve is close to the polymer-solvent axis, it means that coagulant is strong for the casting solution (less thermodynamically stable of casting solution). Worth noting is the concentration dependency of $\chi_{13}$ parameter, which is not consider during the assessment of polymer/solvent/non-solvent systems [45]. The interaction parameter between polymer/non-solvent systems which can be related to the solubility parameter difference, can be calculated from equation below [27]:

$$\Delta\delta = [(\delta_{dp} - \delta_{ds})^2 + (\delta_{pp1} - \delta_{pp2})^2 + (\delta_{hp1} - \delta_{hp2})^2]^{0.5} \quad (3)$$

A smaller Δδ indicates a higher polymer/non-solvent affinity. The difference in solubility parameters between polymer/non-solvents are listed in Table 3.

According to Table 3, the affinity between Extem/non-solvents are in the order: methanol > glycerol > water. It was shown that a polymer/non-solvent system with a low $\chi_{13}$ value is characterized by a binodal line lying close to the polymer/non-solvent axis [33,34].

**Table 3.**
The difference in solubility parameters between polymer and non-solvents.

| Solvents | $\delta_D$ $(MPa)^{1/2}$ | $\delta_P$ $(MPa)^{1/2}$ | $\delta_h$ $(MPa)^{1/2}$ | $\delta_t$ $(MPa)^{1/2}$ | Δ $(MPa)^{1/2}$ |
|---|---|---|---|---|---|
| Extem | 17.01 | 3.66 | 8.27 | 19.27 | N.A. |
| Water | 14.3 | 31.3 | 34.2 | 47.83 | 37.99 |
| Glycerol | 17.3 | 12.1 | 29.3 | 36.11 | 22.66 |
| Methanol | 15.2 | 12.3 | 22.3 | 29.65 | 16.57 |

**Table 4.**
Cloud point data for Extem/solvent/non-solvent systems at 25 °C for 13.5% polymer concentration.

| System | Polymer (%) | Solvent (%) | Non-solvent (%) | Non-solvent/ solvent |
|---|---|---|---|---|
| Water/DMSO | 13.51 | 85.40 | 1.08 | 0.01 |
| Water/DMF | 13.07 | 83.48 | 3.45 | 0.04 |
| Water/DMAc | 13.16 | 81.74 | 5.10 | 0.06 |
| Water/NMP | 13.49 | 78.50 | 8.01 | 0.10 |
| Glycerol/NMP | 13.38 | 70.43 | 16.19 | 0.22 |
| Methanol/ NMP | 13.15 | 67.19 | 19.66 | 0.29 |

Hence, in this case the polymer/non-solvent effect predominates over that of the non-solvent/solvent system. It is known that the phase separation is affected by the coagulation strength, so this analysis could be valuable for choosing suitable coagulants in forming the dope composition. For example for instantaneous demixing, the strongest coagulant, water and for a delayed demixing, methanol should be used. Moreover, the solubility parameter analysis of coagulant/NMP systems reveals that hydrogen bonding is the most important parameter to define the power of various coagulants. Among the studied non-solvents, water has the highest ability to form hydrogen bonding with NMP. Thus, it can be concluded that higher values of $g_{12}$ along with lower values of $\chi_{23}$ and $\chi_{13}$, shift the binodal curve toward the polymer-non-solvent axis, and yield a smaller demixing gap.

For most ternary membrane forming systems, the ratio of non-solvent to solvent at the cloud point does not change significantly with a change in polymer concentration [46]. Thus, this ratio is an approximation of the position of the binodal line. This ratio is given in Table 4 for the studied systems. A higher value means that the cloud point curve is lying more close to the polymer-non-solvent axis and vice versa.

### 3.4. Linearized cloud point correlation (LCP)

A linearized cloud point (LCP) relationship, correlating the concentration of non-solvent to the polymer at the solidification point, was proposed by Boom [47]. The LCP provides quick information about the thermodynamics of the membrane formation process. The LCP plot for each individual polymer/solvent/non-solvent systems can be simply developed, on the following conditions: 1) observation of low affinity between polymer/non-solvent, 2) high affinity between polymer/solvent, resulting in complete miscibility [47,48]. The LCP relation consists of two constant parameters: the slope (a) and the intercept (b) of the line, which should be determined experimentally.

$$\ln\frac{\varnothing 1}{\varnothing 2} = a\ln\frac{\varnothing 2}{\varnothing 3} + b \quad (4)$$

where $ø_1$, $ø_2$, and $ø_3$ are reffered to the weight fraction of the coagulant, solvent, and polymer, respectively, at the cloud point; The slope is determined by following equation:

$$a = \frac{v1 - v3}{v2 - v3} \quad (5)$$

where $v_1$, $v_2$, and $v_3$ are referred to the molar volumes ($m^3$/mol) of the coagulant, solvent, and polymer, respectively. It was reported that the value of a (slope) should be higher than one. However, due to the experimental error this value may become smaller than unity, although always close to one. The intercept (b) gives information about the interaction parameters because both interaction parameters and molar volumes are taken into account. Since all cloud point values are assessed in same way, the polymer/non-solvent interaction parameter is estimated in a superior way [47–49]. Fig. 7 shows the LCP relation of the Extem/NMP/non-solvent ternary systems at room temperature.

The LCP parameters along with the regression coefficient ($R^2$) have been listed in Table 5. This table indicates that the slopes of studied systems are somewhat higher than one.

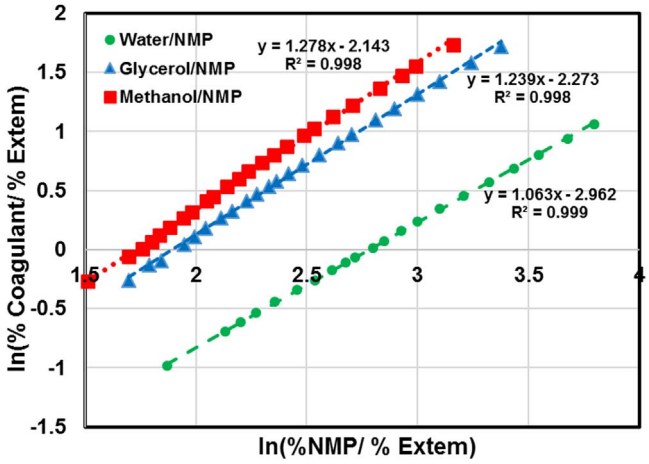


**Fig. 7.** The LCP plot for Extem/non-solvent/NMP systems.

**Table 5**
The LCP relation parameters for Extem/NMP/non-solvent systems.

| Coagulant | Slope (a) | Intercept (b) | Correlation index ($R^2$) |
|---|---|---|---|
| Water/NMP | 1.063 | −2.962 | 0.999 |
| Glycerol/NMP | 1.239 | −2.273 | 0.998 |
| Methanol/NMP | 1.278 | −2.143 | 0.998 |

Moreover, the intercept (b) of the methanol/NMP system is more than that of the water/NMP and glycerol/NMP systems. If the regression coefficient value become very close to one, this means that the experimental cloud points were correlated very well by the LCP relation [49]. The high correlation indices in Table 5 are an indication of well accordance between the LCP relation and the obtained cloud point curves of Extem/NMP/non-solvent systems. The LCP correlation in Fig. 7 again proves that water is a strong coagulant for Extem (strongly incompatible with the water).

### 3.5. Precipitation value (PV)

The term"precipitation value" which was firstly proposed by Wang and TEO [19], is defined as the amount of non-solvent needed to make 2 g polymer (in 100 g solvent) turbid. It was shown that the initial incidence of phase separation in a membrane formation system can be determined by PV. The strength of a non-solvent for a casting solution can be identified by PV. In fact, the PV quantitatively shows the amount of non-solvent needed to start the precipitation at a certain polymer concentration. A lower compatibility of the non-solvent and polymer promotes polymer precipitation. Thus, a higher PV value corresponds to a higher tolerance of polymer solution to the non-solvent [11]. Fig. 8 shows the PV plots for the selected non-solvents versus Extem concentration. In this study, we modified the definition of PV to "the weight of coagulant (g) required to make 100 g of polymer solution cloudy".

Moreover, different Extem concentrations (around between 5–25 wt%) were considered. It can be observed that the power of non-solvents is in the order of water > glycerol > methanol. The PVs of coagulants used again confirm the experimental results. It should be noted that non-solvents having higher $\delta_h$ values (higher hydrogen-bonding ability and therefore better non-solvent/polymer compatibility) show lower PVs [50]. Hence, the PVs for water are significantly lower than those of the alcohols (methanol and glycerol), indicating the low non-solvent tolerance of the Extem/NMP system for water.

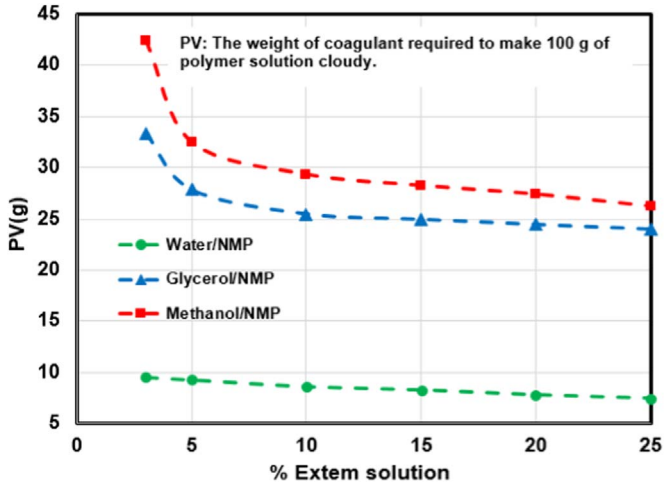


**Fig. 8.** PV versus polymer concentration for water/NMP, glycerol/NMP and methanol/NMP.

### 3.6. Membrane morphology

The parameters affect the final structure of the membrane in the phase inversion process are various and complicated. The most important parameters are the type of solvent and non-solvent, the casting solution concentration, the coagulation bath temperature, the demixing gap location, and additives [9]. In the ternary phase diagram for membrane formation, several different pathways exist which results in different morphologies. After immersion of the casting solution in a coagulation bath, the composition path will follow one of two different routes: a) an instantaneous demixing and b) delayed demixing (Fig. 9).

If in the first moments of immersion (at $t < 1$ s), the binodal line is touched or crossed, liquid-liquid demixing happens in the interfacial region which is denoted as instantaneous demixing. This involves a large inflow of non-solvent, while the outflow of solvent is relatively small. In other words, the ratio of the incoming non-solvent diffusion (into the polymer) to the outward solvent diffusion (into the non-solvent) is high. This type of demixing usually yields a thin skin layer over a porous sub-layer with a finger-like structure containing large void spaces [44,51,52]. The occurrence of macrovoids in the membrane structure has some disadvantages. Although a skin top layer is formed, it usually contains imperfections and mechanical failures which is not suitable for high pressure processes such as gas separation.

In contrast, a low solvent/non-solvent affinity leads to delayed demixing, which occurs if the binodal line is crossed at a later stage (not in the first moments of immersion). In this case, there is a time interval ($t > 1$ s) between the moment of immersion of the casting solution in the non-solvent bath and the onset of demixing. During the delay time, the ratio of the inward non-solvent to the outward solvent diffusion is reduced because of a delay time before the onset of phase separation. The types of solvent and non-solvent used have an important role in the delayed demixing process. It is expected that systems induce delayed demixing exhibit membranes with a relatively dense skin layer along with sponge like sub-layer [51–53]. It was demonstrated that non-solvent/solvent pairs having $\chi_{12} < 1.5$ give instantaneous demixing [8,54]. Based on this fact and the ternary phase diagram (Fig. 4**),** it is expected that all studied systems induce instantaneous demixing which would form finger-like sub structures with a thin top layer. However, no precise predictions of the morphologies of quaternary systems can be made on this basis. Fig. 10 illustrates the morphology of the asymmetric membranes prepared from different water/solvent/Extem systems at room temperature. A thin skin layer over a finger like macrovoids (tear) sub-structure was formed in all the prepared membranes except for the water/DMSO/Extem system. A sponge structure with a thick top layer was observed for the Extem/DMSO/water system. In was found that in the ternary phase diagram, it would be easier to form a dense membrane when there is a smaller demixing gap [54]. Hence, among the studied systems, the water/NMP/Extem system should form a denser top layer compared to other systems. However, as can be observed from Fig. 10, the membrane formed from Extem/DMSO and Extem/NMP solutions actually had a denser and thinner top layer, respectively. This observations is not consistent with the ternary phase diagram results. As shown in Fig. 4, the cloud point curve of water/DMSO/Extem was the closest to the polymer-solvent axis, which suggests the largest demixing gap. Thus, in this system less water is required to percipitate polymer. The sponge structure of Extem/DMSO is due to the fact that in contact with water, a dense top layer was formed immediately, which suppresses the non-solvent/solvent exchange rate, resulting in a sponge like structure [5].

Several studies demonstrated that membranes with a finger-like structure are formed by water/DMSO and water/NMP, irrespective of the polymer type [55–57]. However, a typical sponge-like sub-layer with a relatively uniform pore distribution from Extem/DMSO/water system was obtained in this study. Similarly, Kim et al. [18] observed a membrane with finger-like structure formed by using NMP in the

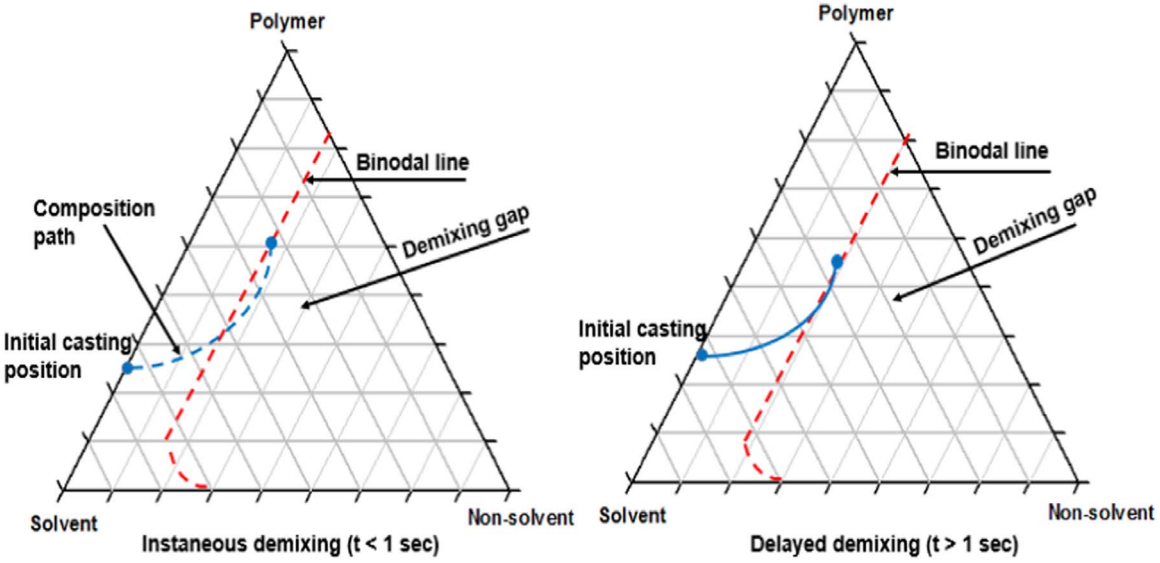


**Fig. 9.** Composition pathways of a cast polymer film during immersion step.

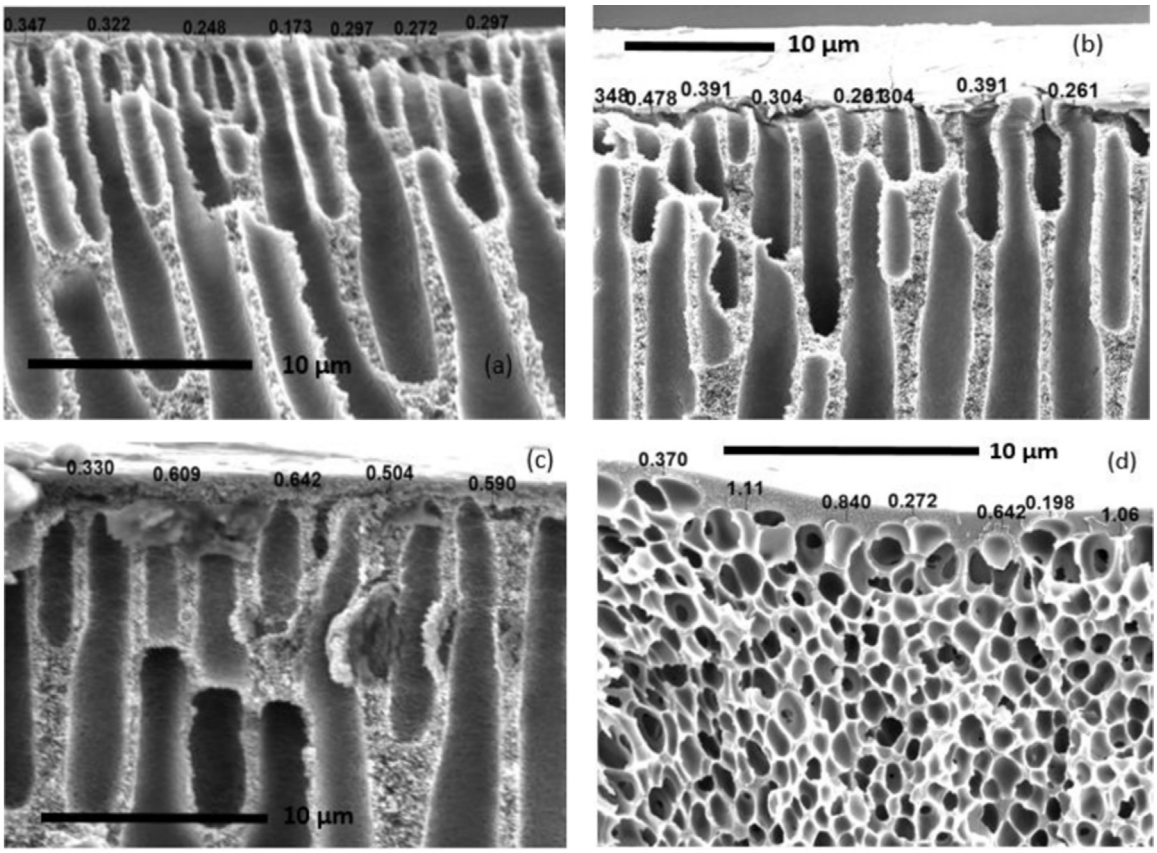


**Fig. 10.** Morphology of the asymmetric membranes prepared from (a) Extem/NMP/water, (b) Extem/DMAc/water (c) Extem/DMF/water and (d) Extem/DMSO/water systems.

casting solution, and water as coagulation bath. By using DMSO in the casting solution a membrane with sponge-like structure was formed via instantaneous demixing.

### 3.7. Factors affecting membrane morphology

Some authors studied the relation of the membrane morphology with the properties of the used forming systems. For this purpose, the thermodynamic and kinematic aspects of the current water/solvent/Extem systems are evaluated in order to determine correlations and simultaneously to give insight into the mechanism of membrane formation.

#### 3.7.1. Solvent/non-solvent interaction

Materials with low interaction parameter values ($g_{12}$) have a higher tendency to form a mixture. It is known that the formation of macrovoids suppresses when there is a low tendency of mixing between non-solvent/solvent. This can be reffered to the non-solvent/solvent interaction parameter [51,52]. As shown in Fig. 5, the $g_{12}$ value of water/NMP is higher than that of water/DMAc and water/DMF over the entire composition, indicating a higher affinity between water/DMAc and water/DMF systems compared to water/NMP. Therefore, smaller fingers (tears) are expected to be observed in membranes formed from water/NMP. Furthermore, as mentioned earlier, water/DMSO (a large negative value of $g_{12}$) has a very low interaction parameter, which indicates a high affinity. This high mutual affinity should induce an instantaneous demixing in this system which typically results in finger-like sub-layer formation [51–53,58]. However, Extem/DMSO/water exhibited delayed demixing, which led to a sponge like structure. Moreover, the average thickness of the membrane skin layer prepared from NMP, DMAc, DMF and DMSO casting solutions is 0.28, 0.34, 0.53 and 0.64 μm, respectively, indicates that with increasing the affinity of non-solvent/solvent the top layer thickness increases.

#### 3.7.2. Polymer/solvent interaction

It was demonstrated that the type of solvent used for the casting solution has an effect on the properties and performance of a membrane formed by phase inversion [16,24]. Hence, in the design of a membrane process, selecting a suitable solvent is crucial. The lower interaction value (higher affinity) between polymer/solvent results in a higher precipitation rate of polymer via the formation of finger-like structures. The interaction parameters for the studied Extem/solvents are in the order: Extem/DMAc > Extem/NMP > Extem/DMF > Extem/DMSO. SEM images of Extem/NMP, Extem/DMAc and Extem/DMF systems exhibited finger-like structures while a sponge-like structure was observed for Extem/DMSO. Moreover, there is no relation between the thickness of the top layers of membranes and the mutual affinity of polymer/solvent. Hence, it can be concluded that polymer/solvent interaction parameters in the studied systems could not significantly change the precipitation conditions.

#### 3.7.3. Heat of mixing

Systems associated with a large heat of mixing typically induce instantaneous demixing and therefore, macrovoid formation. Frommer and Lancet [59] showed that high values of the heat of mixing correspond to high polymer precipitation rates, which helps the finger-like formation. Bottino et al. [60] reported that the size and number of macrovoids reduces as the heat of mixing of solvent/non-solvent becomes less exothermic or more endothermic. The heat of mixing of water/solvent mixtures versus the mole fraction of solvent is shown in Fig. 11. The minimum amount of heat of mixing for the studied solvents follows the order: water/DMAc < water/NMP < water/DMSO < water/DMF. The presence of a minimum in the heat of mixing curves for some water/solvent mixtures can be an indication of

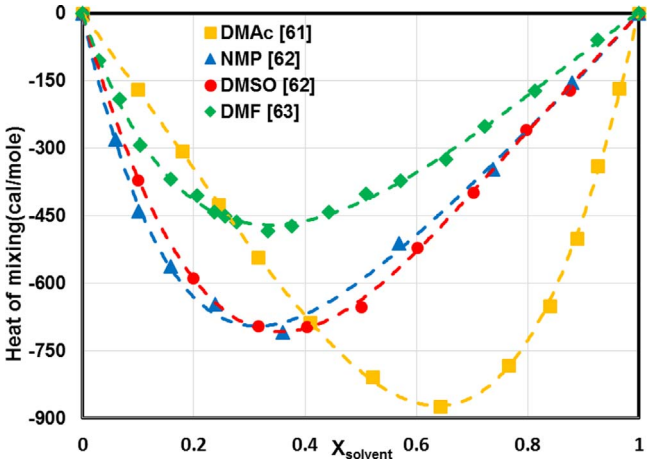


**Fig. 11.** The heat of mixing of water/solvent mixtures as a function of the solvent mole fraction.

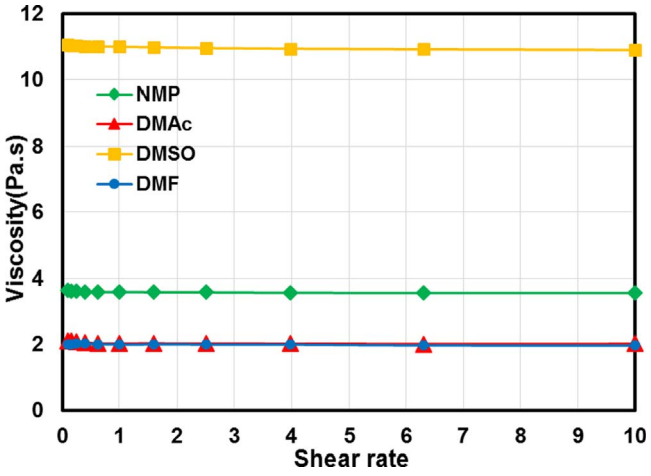


**Fig. 12.** The viscosities of different Extem/solvent polymer solution (25 wt%) at 25 °C.

complex formation, as suggested by Assarsson and Eirich [61]. Formation of complexes was verified by spectroscopic studies from NMR data.

Water molecules are bound to the carbonyl group of NMP. The formation of these complexes increases the viscosity significantly, and decreases the diffusion coefficient. On the other hand, the molecular interactions between water/NMP appear stronger than intermolecular interaction between similar pairs. Consequently, water/NMP mixing induces a large exothermic heat which significantly increases the temperature (about 25 °C) and thus, thermal diffusion is facilitated by the developed heat [62,64,65]. The heat of mixing between NMP and water is large (Fig. 11), the membrane is formed more quickly and has a finger-like macrovoid structure.

The DMSO/water system has similar characteristics to the NMP/water system. Due to the hydrogen bond formation between water/DMSO (basic portion of DMSO via its oxygen atom and the acid portion of water via its protons), a large exothermic heat would be released and the complex compound (1 mol DMSO with 2 mol $H_2O$) would be formed [62,66,67]. Hence, in water/DMSO system, due to the rapid formation of a dense layer the formation of a finger-like structure is avoided.

The water/DMF mixing process is exothermic which is a consequence of: (i) polar and strongly basic carbonyl group with water molecules; (ii) the repulsive interaction between the hydrophobic groups (CH) and water. The second consequence causes an energy release [63,68]. Petersen [69] showed that the mixing of DMF with water induced the heat over the entire concentration range, by the formation of hydrogen bonds between water molecules and carbonyl oxygen. It can be concluded that a prediction of the final membrane structure using heat of mixing between non-solvent/solvent seems challenging.

### 3.7.4. Viscosity

The viscosity of the dope solution can strongly affect the non-solvent/solvent exchange and therefore, the velocity of phase separation [64]. It was generally found that a high viscosity of the casting solution hinders the penetration of the non-solvent into the casting solution during the phase inversion process, and thus the possibility of macrovoids formation is reduced [5]. Friedrich et al. [70] discovered that the amount of cavity formation in the morphology of the membrane is a function of polymer solution viscosity. Experimental viscosities of different Extem/solvent polymer solutions at 25 °C at shear rate between 0 and 10 1/s are shown in Fig. 12 and listed in Table 6.

It is obvious that the viscosity of Extem/DMSO solutions (~11 Pa s) is much higher than that of other Extem/solvent solutions, which

**Table 6**
Experimental viscosities of different Extem/solvent polymer solution (25 wt%) at 25 °C.

| Polymer/solvent System | Viscosity (Pa.s) |
|---|---|
| Extem/NMP | 3.6 |
| Extem/DMAc | 2.06 |
| Extem/DMF | 2.02 |
| Extem/DMSO | 11.01 |

results in a higher resistance of mass transfer during the percipitation process.

High viscosity of polymer solution promote the kinetic hindrance with suppress the thermodynamic factors. This leads to formation of a membrane with thick sponge-like sublayer. Moreover, the possibility of a finger-like structure formation due to the high viscosity of the casting solution is decreased. Hence, according to data obtained from viscosity measurements, Extem/DMAc and Extem/DMF systems must show more macrovoids in their structure compared to the Extem/NMP system, while the high viscosity of DMSO can further lead to the formation of the observed sponge-like structure of the Extem/DMSO/water system.

### 3.7.5. Diffusion rate

The exchange rate between solvent in the polymer film and non-solvent in the coagulation bath is determined by the kinetics and depends on the exchange rate. It is known that in some cases mass transfer can control the mechanism of the membrane forming system. However, because of the simultaneous mass and heat transfer during phase inversion, quantifying the importance of mass transfer is a complex process [71–73]. During membrane formation in the very first moments of the immersion, solvent and non-solvent start to diffuse mutually just before polymer diffusion occurs and membrane skin forms. The diffusivity for the polymer in solution is at least one order of magnitude smaller than the diffusivity of solvent and non-solvent ($D \sim 10^{-5}$ $cm^2$/sec). The membrane structure (local concentration of different species) depends on the solvent/non-solvent diffusion rate [73–78]. Therefore, the binary diffusivity of solvent/non-solvent can give more understanding of the formation process. Wilke-Chang [79] proposed a simple prediction for determination of diffusivity of water in solvent and solvent in water:

$$Da - b = 7.4 \times 10^{-8} \frac{(xMb)^{\frac{1}{2}} T}{\eta b Va^{0.6}} \quad (6)$$

where $D_{a\text{-}b}$ ($cm^2$/sec) is the mutual diffusivity of component a in component b, T (K) is the absolute temperature, $M_b$ is the molecular

**Table 7**
Diffusion coefficient values for different solvent/water systems at 25 °C [80].

| Solvent | Ds-w (Solvent/Water) ($10^{-6}$ $cm^2$/sec) | Dw-s (Water/Solvent) ($10^{-6}$ $cm^2$/sec) | $D_m$ ($10^{-6}$ $cm^2$/sec) |
|---|---|---|---|
| NMP | 8.9 | 9.3 | 9.1 |
| DMAc | 9.1 | 16.8 | 11.8 |
| DMF | 10.2 | 17.1 | 12.8 |
| DMSO | 10.7 | 6.9 | 8.4 |

mass of component b; $V_a$ ($cm^3$/mole) is the molar volume of component a, $\eta$ (Pa. S) is the absolute viscosity; and x is the association factor. Eq. (5) is a satisfactory correlation for estimation of diffusion coefficients with good enough accuracy for most engineering purposes. Table 7 presents the diffusion coefficient values for different solvent/water systems at 25 °C, together with the harmonic mean value of average diffusion:

$$Dm = \frac{2Ds - w.Dw - s}{Ds - w + Dw - s} \quad (7)$$

$D_m$ can give a more precise value than the average value for diffusion of solvent in non-solvent and vice versa.

During the phase inversion, if the exchange rate of solvent and non-solvent is low (because of a lower diffusion coefficient), it takes more time before sufficient solvent is taken out of the polymer solution to occur demixing. Hence, when the diffusivity of the solvent in the non-solvent bath is low or the diffusivity of the non-solvent in the polymer solution is low, delayed demixing may take place. From Table 7, it is clear that the order of $D_m$ for the studied water/solvent systems is in the order: DMF > DMAc > NMP > DMSO. The rate of water diffusion primarily depends on the viscosity of the polymer solution. For DMSO, due to the high interaction with water, a dense layer forms immediately which hinders the solvent exchange process. A low diffusion rate of DMSO/water along with a high viscosity of the polymer solution increases the solvent exchange process time, which results in a sponge-like structure. As overall conclusion, the diffusion rate has a significant influence on the final membrane morphology.

## 4. Effect of different coagulants on membrane morphology

The type of non-solvent can lead to the transition from instantaneous to delayed demixing. The cross-section morphology of the membranes prepared from Extem/NMP/methanol and Extem/NMP/glycerol systems is shown in Fig. 13. Using methanol as a coagulation medium results in a thick dense layer over a macroporous sub layer while a fully sponge-like structure with microporous skin layer was observed in the Extem/NMP/glycerol system.

Several parameters already mentioned above are discussed here.

**Table 8**
The viscosities, and diffusion coefficients for non-solvent/NMP systems at 25 °C [44,81,82].

| Coagulant | Viscosity (cP) | D (NMP/non-solvent) ($10^{-6}$ $cm^2$/sec) | D (non-solvent/NMP) ($10^{-6}$ $cm^2$/sec) | $D_m$ ($10^{-6}$ $cm^2$/sec) |
|---|---|---|---|---|
| Water | 1 | 8.7 | 18 | 11.73 |
| Glycerol | 945 | 0.02 | 9 | 0.03 |
| Methanol | 0.6 | 16.2 | 12.6 | 14.17 |

Table 8 presents the viscosities and binary diffusion coefficients of studied non-solvent/NMP systems at 25 °C. The $D_m$ value of NMP/methanol is higher than the $D_m$ value of NMP/water, which causes a rapid interchange of solvent and non-solvent typically leading to instantaneous demixing. Moreover, the lower viscosity of methanol compared to water facilitates the miscibility of NMP with methanol and the demixing process.

Hence, based on kinematic properties (higher diffusivity and lower viscosity than water), Extem/NMP/methanol should induce instantaneous demixing and thus, a membrane including a thin dense layer with a porous support layer was expected. However, SEM images showed a thick dense layer with a macroporous sub-structure. With increasing mutual affinity of solvent/non-solvent and polymer/non-solvent, the possibility formation of a sponge-like structure decreases. This difference of affinity can be reffered to the interaction parameters. Based on the ternary phase diagram (Fig. 6), it is expected that unlike the Extem/NMP/water system, Extem/NMP/methanol and Extem/NMP/glycerol would exhibit delayed demixing. From Table 3, it is clear that the interactions of Extem/non-solvent systems are in the order Extem/water > Extem/glycerol > Extem/methanol. Due to the lower interaction between polymer/methanol, the binodal line of Extem/NMP/methanol is moved toward the polymer non-solvent axis which resulted in the observed morphology. Thus, for this system, the influence of the thermodynamic properties by means of non-solvent/polymer interaction predominates over those kinematic effects (viscosity and diffusivity) of the non-solvent/solvent system.

In Fig. 6 the cloud point line of the Extem/NMP/glycerol system on the ternary phase diagram is very close to Extem/NMP/methanol. Thus, a similar structure for Extem/NMP/glycerol was expected based on the ternary phase diagram. However, a super porous structure was observed for this system. In comparison with methanol, the $D_m$ value of NMP/glycerol is very low (Table 8). The higher viscosity of glycerol compared to methanol causes a higher resistance of mass transfer during the immersion step. Due to the high viscosity of glycerol, slow diffusion of glycerol into the polymer solution occurs. Therefore, the rate of crystallization is very low and glycerol could flow into the membrane. During the phase-separation process of this system many

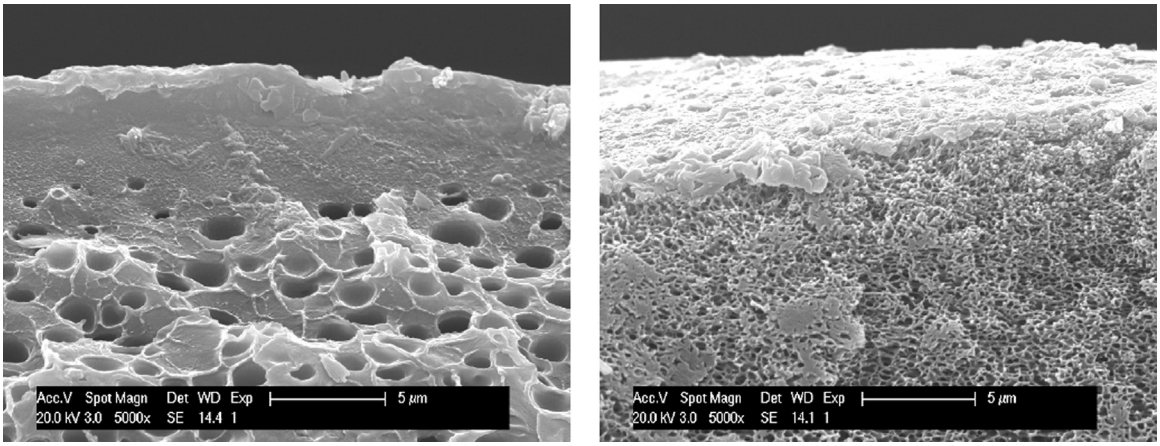


**Fig. 13.** The cross-section morphology of the membranes prepared from Extem/NMP/methanol and Extem/NMP/glycerol.

micropores raised simultaneously by diffusion of NMP to glycerol and glycerol to the polymer solution. The pore size of the sub-layer is therefore comparatively small. The effect of Extem/NMP/glycerol on the membrane morphology is more related to its kinematic properties (viscosity and diffusivity), which further delayed the non-solvent influx. The kinetic hindrances due to viscosity overcame the thermodynamic factor and thus lead to formation of a fully developed sponge-like structure. Thus, unlike Extem/NMP/methanol for this system kinematic properties are controlling parameters.

## 5. Conclusion

In present study, the phase separation behavior of the Extem dope solution was evaluated for four aprotic solvents, i.e., NMP, DMF, DMAc and DMSO and three different types of coagulants, including water, methanol and glycerol, through cloud point measurements. The membrane's morphologies formed from different systems was investigated by SEM. To clarify the mechanisms of membrane formation, the kinetics and thermodynamics aspects of the phase separation were studied. It was observed that membranes formed from Extem/NMP/water, Extem/DMAc/water and Extem/DMF/water systems exhibited an instantaneous demixing which led to the formation of finger like macrovoids, while Extem/DMSO/water showed a different structure. In spite of the higher mutual affinity between water/DMSO than the other water/solvents, membranes formed from DMSO have a sponge-like structure. Instantaneous formation of dense layer suppresses the solvent exchange process. Furthermore, due to the lower diffusivity value of DMSO/water and the higher viscosity of the polymer solution, solvent exchange process occurs at a lower rate in comparison with the other systems. It was believed that for different Extem/solvent/water systems, both thermodynamic and kinetic aspects have prominent effect on the final structure of the membranes.

Furthermore, the influence of different non-solvents (methanol and glycerol) on the morphology of membranes was studied in detail. An unexpected morphology was achieved for both non-solvents. Based on kinematic properties (diffusivity and viscosity), an instantaneous demixing with porous structure was expected for this system. Formation of a dense membrane in the methanol coagulation bath was suggested to be due to the importance of thermodynamic parameters. For Extem/NMP/glycerol system an opposite structure was observed in SEM images. A membrane with macroporous structure was formed due to the importance of kinetic parameters. A high viscosity of glycerol along with a low diffusivity (low $D_m$) delayed the solvent exchange process along with the formation of a micropore structure.

## Acknowledgment

The author gratefully acknowledge Anja Vananroye (Department of Chemical Engineering, KU Leuven) for measuring the viscosity of polymer solutions.

## Appendix A

### 6.1. A.1. Polymer-solvent binary interaction parameters

The Hansen Solubility Parameter (HSP) has proven to be a practical method to express the nature and magnitude of the interaction forces between the polymer/solvent. According to the HSP, polymers and solvents with a small difference in solubility parameters tend to be miscible. The HSP is made up of three individual components [27]:

$$\delta_t = \delta_d + \delta_p + \delta_h \tag{A.1}$$

These parameters present the individual contribution of the dispersion bonding ($\delta_d$), polar bonding ($\delta_p$), and hydrogen bonding ($\delta_h$) forces between molecules. HSP values are known for only a limited number of polymers.

Group contribution is a reliable method to predict the HSP values for polymers based on their chemical structures. Solubility parameters of complex structures that typically happen in multi-ring polymers can be predicted simply based on their chemical structure. The structure of a polymer is first divided into its group components and then numerical values are assigned to each of them. Using these numerical values, the three partial solubility parameters and the overall solubility parameter can be calculated when the chemical structure of the repeating unit of polymer is known. In this work, the HSP of the polymers were calculated using the Hoftyzer-Van Krevelen approach [31]:

$$\delta_d = \frac{\sum F_{di}}{\sum V_i} \tag{A.2}$$

$$\delta_p = \frac{\sqrt{\sum F_{pi}^2}}{\sum V_i} \tag{A.3}$$

$$\delta_h = \sqrt{\frac{\sum E_{hi}}{\sum V_i}} \tag{A.4}$$

$$\delta = \sqrt{\delta_d^2 + \delta_p^2 + \delta_h^2} \tag{A.5}$$

The numerical values assigned to each structural group of polymer are tabulated in Table A.1.

**Table A.1**
Calculation of Hansen solubility parameters for studied polymers by using Hoftyzer-van Kervelen method.

| Structural groups | No. groups | $F_{di}$ ($J^{1/2}$ $cm^{3/2}$ $mol^{-1}$) | $F_{pi}$ ($J^{1/2}$ $cm^{3/2}$ $mol^{-1}$) | $F_{hi}$ ($J.mol^{-1}$) | V ($cm^3mol^{-1}$) |
|---|---|---|---|---|---|
|  | 4 | 1270 | 110 | 0 | 65.5 |
| 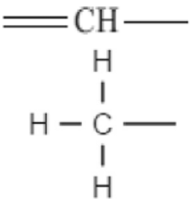 | 6 | 200 | 0 | 0 | 13.8 |
| | 2 | 420 | 0 | 0 | 23 |
| 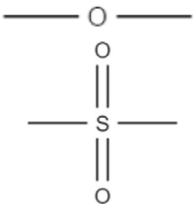 | 2 | 100 | 400 | 3000 | 3.8 |
| | 1 | 591 | 0 | 13490 | 32.5 |
|  | 1 | −70 | 0 | 0 | 5.32 |
| 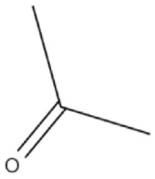 | 4 | 290 | 770 | 2000 | 13.6 |
| 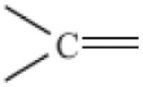 | 4 | 70 | 0 | 0 | 8 |
| 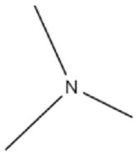 | 2 | 20 | 800 | 5000 | 12.6 |

## References


[1] R.W. Baker, Membrane technology and applications, John Wiley & Sons, Ltd, West Sussex, England, 2004.
[2] M. Khayet, T. Matsumura, Membrane distillation: principles and applications, Elsevier, Oxford, U.K, 2011.
[3] D.-M. Wang, J. Lai, Recent advances in preparation and morphology control of polymeric membranes formed by nonsolvent induced phase separation, Curr. Opin. Chem. Eng. 2 (2013) 229–237.
[4] B. Singh Lalia, V. Kochkodan, R.H.N. Hilal, A review on membrane fabrication: structure, properties and performance relationship, Desalination 326 (2013) 77–95.
[5] N. Hilal, A.F. Ismail, Ch Wright, Membrane Fabrication, CRC Press, 2015, p. 02.
[6] G.R. Guillen, Y. Pan, M. Li, E.M.V. Hoek, Preparation and characterization of membranes formed by nonsolvent induced phase separation: a review, Ind. Eng. Chem. Res. 50 (2011) 3798–3817.
[7] K. Boussu, B. Van der Bruggen, C. Vandecasteele, Evaluation of self-made nanoporous polyethersulfone membranes, relative to commercial nanofiltration membranes, Desalination 200 (2006) 416–418.
[8] P. Menut, Y.S. Su, W. Chinpa, C. Pochat-Bohatier, A. Deratani, D.M. Wang, P. Huguet, C.Y. Kuo, J.Y. Lai, C. Dupuy, A top surface liquid layer during membrane formation using vapor-induced phase separation (VIPS)-Evidence and mechanism of formation, J. Membr. Sci. 310 (2008) 278–288.
[9] M. Mulder, Basic Principles of MembraneTechnology, 2nd ed, Kluwer Academic, Dordrecht, Boston, 1996.
[10] H. Strathmann, Preparation of microporous membranes by phase inversion processes, in: E. Drioli, M. Nakagaki (Eds.), Membranes and Membrane Processes,

Plenum, New York, NY, 1986, p. 115.
[11] C.A. Smolders, A.J. Reuvers, R.M. Boom, I.M. Wienk, Microstructures in phase-inversion membranes, Part 1. formation of macrovoids, J. Membr. Sci. 73 (1992) 259–275.
[12] P. van de Witte, P.J. Dijkstra, J.W.A. van den Berg, J. Feijen, Phase separation processes in polymer solutions in relation to membrane formation, J. Membr. Sci. 117 (1996) 1–31.
[13] H. Ohya, V. Kudryavsev, S.I. Semenova, Polyimide membranes: applications, fabrications and properties, Gordon and Breach publishers, CRC Press, Tokyo, 1996
[14] J.G. Wijmans, J. Kant, M.H.V. Mulder, C.A. Smolders, Phase separation phenomena in solutions of polysulfone mixtures of a solvent and a non-solvent: relationship with membrane formation, Polymer 26 (1985) 1539–1545.
[15] A.K. Hołda, Ivo F.J. Vankelecom, Understanding and guiding the phase inversion process for synthesis of solvent resistant nanofiltration membranes, J. Appl. Polym. Sci. 132 (2015) 42130.
[16] H. Strathmann, K. Kock, The formation mechanism of phase inversion membranes, Desalination 21 (1977) 241–255.
[17] H.K. Lonsdale, The growth of membrane technology, J. Membr. Sci. 10 (1982) 81–181.
[18] J.H. Kim, B.R. Min, J. Won, H.Ch Park, Y.S. Kang, Phase behavior and mechanism of membrane formation for polyimide/DMSO/water system, J. Membr. Sci. 187 (2001) 47–55.
[19] D. Wang, K. LI, W.K. Teo, Phase separation in polyetherimide/solvent/nonsolvent systems and membrane formation, J. Appl Polym. Sci. 71 (1999) 1789–1796.
[20] N. Leblanc, D.L. Cerf, C. Chappey, D. Langevin, M. Me´tayer, G. Muller, Influence of solvent and non-solvent on polyimide asymmetric membranes formation in relation to gas permeation, Sep. Purif. Technol. 22 (2001) 277–285.
[21] J. Barzin, B. Sadatnia, Correlation between macro void formation and the ternary phase diagram for polyethersulfone membranes prepared from two nearly similar solvents, J. Membr. Sci. 325 (2008) 92–97.
[22] Ch Yin, J. Dong, Zh Li, Z. Zhang, Q. Zhang, Ternary phase diagram and fiber morphology for nonsolvent/DMAc/polyamic acid systems, Polym. Bull. 72 (2015) 1039–1054.
[23] ⟨https://www.sabic-ip.com/gep/Plastics/en/ProductsAndServices/ProductLine/Extem.html⟩
[24] H. Strathmann, Synthetic membranes and their preparation, in: P.M. Bungay (Ed.) Synthetic membranes: science, Engineering and Applications, D. Reidel, Dordrecht, 1986, pp. 1–37.
[25] R.M. Boom, T. Van den Boomgaard, C.A. Smolders, Equilibrium thermodynamics of a quaternary membrane-forming system with two polymers. 1. calculations, Macromolecules 27 (1994) 2034–2040.
[26] K.Y. Chun, S.H. Jang, H.S. Kim, Y.W. Kim, H.S. Han, Y.I. Joe, Effects of solvent on the pore formation in asymmetric 6FDA-4, 4, ODA polyimide membrane: terms of thermodynamics, precipitation kinetics, and physical factors, J. Membr. Sci. 169 (2000) 197–214.
[27] Ch.M. Hansen, , Second editionHandbook: “Hansen Solubility Parameters: A User's Handbook” 208, CRC Press, Inc., Boca Raton FL, 1999 (shown)( 2007).
[28] J.W.V. Dyk, H.L. Frlsch, D.T. Wu, solubility, Solvency, and solubility parameters, Ind. Eng. Chem. Prod. Res. Dev. 24 (1985) 473–478.
[29] J.J. Florio, D.J. Miller, Handbook of Coating Additives, RC Press, Technology & Engineering, Marcel, 2004.
[30] E.B. Bagley, T.P. Nelson, J.M. Scigliano, Three-dimensional solubility parameters and their relationship to internal pressure measurements in polar and hydrogen bonding solvents, J. Paint Technol. 43 (1971) 35–42.
[31] D.W. Van, Krevelen Revised by K. Te Nijenhuis, Properties of Polymers– Cohesive Properties and Solubility, Fourth edition (2009), 2009.
[32] W.L. Archer, Determination of Hansen solubility parameters for selected cellulose ether derivatives, Ind. Eng. Chem. Res. 30 (1991) 2292–2298.
[33] R. Bloch, M.A. Frommer, The mechanism for formation of ‘skinned’ membranes. I. structure and properties of membranes cast from binary solutions, Desalination 7 (1970) 259.
[34] M.A. Frommer, I. Feiner, O. Kedem, R. Bloch, The mechanism for formation of ‘skinned membranes. II. Equilibrium properties and osmotic flows determining membrane structure, Desalination 7 (1970) 393.
[35] M. Guillotin, C. Lemoyne, C. Noel, L. Monnerie, Physicochemical processes occurring during the formation of cellulose diacetate membranes. Research of criteria for optimizing membrane performance. IV. Cellulose diacetate-acetone-additive casting solutions, Desalination 21 (1977) 165.
[36] M.A. Frommer, R.M. Messalem, Mechanism of membrane formation. VI. convective flows and large void formation during membrane precipitation, Ind. Eng. Chem. Prod. Res. Dev. 12 (1973) 328–333.
[37] P. Neogi, Mechanism of pore formation in reverse osmosis membranes during the casting process, AIChE J. 29 (1983) 402–410.
[38] S.C. Pesek, W.J. Koros, Aqueous quenched asymmetric polysulfone membranes prepared by dry/wet phase separation, J. Membr. Sci. 81 (1993) 71–88.
[39] L. Zeman, G.J. Tkacik, Thermodynamic analysis of a membrane-forming system water/N-methyl-2-pyrrolidone/polyethersulfone, J. Membr. Sci. 36 (1988) 119–140.
[40] R. Dong, J. Zhao, Y. Zhang, D. PAN, Morphology control of polyacrylonitrile (PAN) fibers by phase separation technique, J. Polym. Sci. B Polym. Phys. 47 (2009) 261–275.
[41] Th Lindvig, M.L. Michelsen, G.M. Kontogeorgis, A flory-huggins model based on the Hansen solubility parameters, Fluid Phase Equilibria. 203 (2002) 247–260.
[42] J.A. Gonzalez, A.M. Mayes, Phase behavior prediction of ternary polymer mixtures, Macromolecules 36 (2003) 2508–2515.
[43] A.M.W. Bulte, E.M. Naafs, F. van Eeten, M.H.V. Mulder, C.A. Smolders, H. Strathmann, Equilibrium thermodynamics of the ternary membrane-forming system nylon, formic acid and water, Polymer 37 (1996) (1996) 1647–1655.
[44] J.A. van't Hof, A.J. Reuvers, R.M. Boom, H.H.M. Rolevink, C.A. Smolders, Preparation of asymmetric gas separation membranes with high selectivity by a dual-bath coagulation method, J. Membr. Sci. 70 (1992) 17–30.
[45] J. Barzin, B. Sadatnia, Theoretical phase diagram calculation and membrane morphology evaluation for water/solvent/polyethersulfone systems, Polymer 48 (2007) 1620.
[46] W.F.C. Kools, Membrane formation by phase inversion in multicomponent polymer systems mechanisms and morphologies (PhD thesis), University of Twente, 1968.
[47] R.M. Boom, Th Van den Boomgaard, J.W.A. Van den Berg, C.A. Smolders, Linearized cloudpoint curve correlation for ternary systems consisting of one polymer, one solvent and one non-solvent, Polymer 34 (1993) 2348–2356.
[48] Sh Li, Preparation of hollow fibre membranes gas separations (PhD Thesis), University of Twente, 1994.
[49] L. Shen, Zh Xu, Y. Xu, Phase separation behavior of poly(ether imide)/n,ndi-methylacetamide/nonsolvent systems, J. Appl. Polym. Sci. 89 (2003) 875–881.
[50] G. Wypych, Handbook of Solvents, Chem tech publishing, New York, 2001.
[51] A.K. Pabby, S.H. Rizvi, A.M. Sastre, Handbook of Membrane Separations: chemical, PharmaceuticalFood, and Biotechnological Applications, Second edition, CRC Press, New York, 2015.
[52] I.M. Wienk, R.M. Boom, M.A.M. Beerlage, A.M.W. Bulte, C.A. Smolders, H. Strathmann, Recent advances in the formation of phase inversion membranes made from amorphous or semi-crystalline polymers, J. Membr. Sci. 113 (1996) 361–371.
[53] J. Shieh, T.Sh Chung, , Effect of liquid-liquid demixing on the membrane morphology, gas permeation, thermal and mechanical properties of cellulose acetate hollow fibers, J. Membr. Sci. 140 (1998) 67–79.
[54] P.S.T. Machado, A.C. Habert, C.P. Borges, Effect of liquid-liquid demixing on the membrane morphology, gas permeation, thermal and mechanical properties of cellulose acetate hollow fibers, J. Membr. Sci. 140 (1998) 67–79.
[55] B.F. Barton, J.L. Reeve, A.J. Mchugh, Observations on the dynamics of nonsolvent-induced phase-inversion, J. Polym. Sci., Polym. Phys. 35 (1997) 569–585.
[56] L.W. Chen, T.H. Young, Effect of nonsolvents on the mechanism of wet-casting membrane formation from EVAL copolymers, J. Membr. Sci. 59 (1991) 15–26.
[57] H.C. Shih, Y.S. Yeh, H. Yasuda, Morphology of microporous poly(vinylidene fluoride) membranes studied by gas permeation and scanning electron microscopy, J. Membr. Sci. 50 (1990) 299–317.
[58] A.J. Reuvers, F.W. Altena, C.A. Smolders, Demixing and gelation behavior of ternary cellulose acetate solutions, J. Polym. Sci. B: Polym. Phy. 24 (1986) 793–804.
[59] M. Frommer, D. Lancet, The mechanism of membrane formation: membrane structures and their relation to preparation conditions, in: H.K. Lonsdale, H.E. Podall (Eds.), Reverse Osmosis Membrane Research, Plenum, New York, 1972, p. 85.
[60] A. Bottino, G. Camera-Rodab, G. Capannelli, S. Munari, The formation of microporous polyvinylidene difluoride membranes by phase separation, J. Membr. Sci. 57 (1991) l–20.
[61] P. Assarsson, Y. Eirich, Interaction of water with alkyl-substituted amides, molecular association in biological and related systems, advances in chemistry, American Chemical Society, 1968, pp. 1–11.
[62] D. Macdonald, D. Dunay, G.H. Hyne, Properties of the n-methyl-2-pyrrolidinone-water system, Can. J. Chem. Eng. 49 (1971) 420–423.
[63] M. Cilense, A.V. Benedetti, D.R. Vollet, Thermodynamic properties of liquid mixtures II. Dimethylformamide-water, Thermochim. Acta 63 (1983) 151–156.
[64] H. Yanagishita, T. Nakane, H. Yoshitome, Selection criteria for solvent and gelation medium in the phase inversion process, J. Membr. Sci. 89 (1994) 215–221.
[65] J. Lee, I. Gomez, J.C. Meredith, Non-dlvo silica interaction forces in NMP-water mixtures. I. A Symmetric System, Langmuir 27 (2011) 6897–6904.
[66] J.M.G. Cowie, P.M. Toporov, Assocation in the binary liquid system dimethyl sulphoxide-water, Can. J. Chem. 30 (1961) 2240–2245.
[67] K. Burke, C. Riccardi, Th Buthelezi, Thermosolvatochromism of nitrospiropyran and merocyanine free and bound to cyclodextrin, J. Phys. Chem. B 116 (2012) 2483–2491.
[68] J.M. Cordeiro, L.C.G. Freitas, Study of water and dimethylformamide interaction by computer simulation, J. Phys. Sci. 54 (1999) 110–116.
[69] R.C. Petersen, Interactions in the binary liquid system n-dimethylacetamide-water: viscosity and density, J. Phys. Chem. 64 (1960) 184–185.
[70] G. Friedrich, A. Driancourt, C. Noel, L. Monnerie, Asymmetric reverse osmosis and ultrafiltration embranes prepared from sulfonated polysulfone, Desalination 36 (1981) 39–62.
[71] D. Bouyer, W. Werapun, C. Pochat-Bohatier, A. Deratani, Morphological properties of membranes fabricated by VIPS process using PEI/NMP/water system: SEM analysis and mass transfer modelling, J. Membr. Sci. 349 (2010) 97–112.
[72] S. Pereira Nunes, K. Peinemann, Membrane Technology: in the Chemical Industry, John Wiley & Sons, 2006 (Second, revised and extended edition).
[73] T.C. Shen, I. Cabasso, Ethylcellulose anisotropic membranes, in: R.B. Seymour, G.A. Stahl (Eds.), Macromolecular Solutions, Pergamon, New York, NY, 1982, p. 108.
[74] G. Guarino, O. Ortona, R. Sartorio, V. Vitagliano, Diffusion, viscosity, and refractivity data on the systems dimethylformamide-water and N-methylpyrrolidone-water at 5 °C, J. Chem. Eng. Data 30 (1985) 366–368.
[75] C. Della Volpe, G. Guarino, R. Sartorio, V. Vitagliano, Diffusion, viscosity, and refractivity data on the system dimethylformamide-water at 20 and 40, J. Chem. Eng. Data 31 (1986) 37–40.

[76] D.R. Paul, Diffusion during the coagulation step of wet-spinning, J. Appl. Polym. Sci. 12 (1968) 383–402.
[77] C. Cohen, G.B. Tanny, S. Prager, Diffusion-controlled formation of porous structure in ternary polymer systems, J. Polym. Sci., Polym. Phys. Ed. 17 (1979) 477–489.
[78] I. Cabasso, E. Klein, J.K. Smith, Polysulphne hollow fibers. II, Morphol., J. Appl. Polym. Sci. 21 (1977) 165–180.
[79] C.R. Wilke, P. Chang, Correlation of diffusion coefficients in dilute solutions, AIChE J. 1 (1955) 264–270.
[80] A.F.M. Barton, Handbook of Solubility Parameters and Other Cohesion Parameters, CRC Press, Boca Raton, FL, 1983, p. 153.
[81] Industrial Solvents Handbook, in: E.W. Flick (Ed.)Noyes Data Corporation3rd edn, Park Ridge, NJ, 1985.
[82] R.C. Weast (Ed.)Handbook of Chemistry and Physics57th edn., CRC Press, Inc., Boca Raton, FL, 1976, p. 77.